

# Supercooled liquids and the glass transition

Pablo G. Debenedetti\* & Frank H. Stillinger†‡

\*Department of Chemical Engineering and ‡Princeton Materials Institute, Princeton University, Princeton, New Jersey 08544, USA  
(e-mail: pdebene@princeton.edu)

†Bell Laboratories, Lucent Technologies, Murray Hill, New Jersey 07974, USA

Glasses are disordered materials that lack the periodicity of crystals but behave mechanically like solids. The most common way of making a glass is by cooling a viscous liquid fast enough to avoid crystallization. Although this route to the vitreous state — supercooling — has been known for millennia, the molecular processes by which liquids acquire amorphous rigidity upon cooling are not fully understood. Here we discuss current theoretical knowledge of the manner in which intermolecular forces give rise to complex behaviour in supercooled liquids and glasses. An intriguing aspect of this behaviour is the apparent connection between dynamics and thermodynamics. The multidimensional potential energy surface as a function of particle coordinates (the energy landscape) offers a convenient viewpoint for the analysis and interpretation of supercooling and glass-formation phenomena. That much of this analysis is at present largely qualitative reflects the fact that precise computations of how viscous liquids sample their landscape have become possible only recently.

**T**he glassy state is ubiquitous in nature and technology<sup>1</sup>. It is crucial in the processing of foods<sup>2</sup>, the commercial stabilization of labile biochemicals<sup>3</sup>, and the preservation of insect life under extremes of cold or dehydration<sup>3</sup>.

Window glass, composed mostly of sand, lime and soda, is the best-known example of an engineered amorphous solid<sup>4</sup>. Optical fibres are made of very pure amorphous silica, occasionally carefully doped. Most engineering plastics are amorphous solids, as are some metallic glasses and alloys of interest because of their soft magnetism and corrosion resistance<sup>5</sup>. The silicon used in many photovoltaic cells is amorphous, and it is possible that most water in the Universe may be glassy<sup>6</sup>. Most of these examples entail supercooling of a liquid to take advantage of viscous retardation of nucleation and crystallization. Understanding quantitatively the extraordinary viscous slow-down that accompanies supercooling and glass formation is a major scientific challenge<sup>7</sup>.

We begin by reviewing the phenomenology of vitrification and supercooling. A useful approach for relating this complex phenomenology to molecular-scale events is to focus attention on the liquid's energy landscape, that is, the multidimensional surface generated by the system's potential energy as a function of molecular coordinates. Accordingly, basic landscape concepts and a discussion of the important theoretical and computational progress currently being made in this area are presented next. This is followed by a discussion of alternative viewpoints, in which narrowly avoided singularities are assumed to occur well above the glass-transition temperature. We then close with a summary of the important open questions.

It is impossible to do justice to the entire field of supercooled liquids and amorphous solids in an article of this length. We have therefore limited the scope to the dynamics and thermodynamics of viscous liquids above and close to the glass-transition temperature  $T_g$  — in other words, to the glass transition viewed 'from the liquid'. The view 'from the solid', including such topics as relaxation both relatively near

(for example, during annealing or ageing) and far below  $T_g$ , is not discussed. The reader is referred to an excellent recent review<sup>8</sup> for a thorough coverage of these and other topics.

## Phenomenology of supercooling and glass formation

Figure 1 illustrates the temperature dependence of a liquid's volume (or enthalpy) at constant pressure<sup>4,9</sup>. Upon cooling below the freezing point  $T_m$ , molecular motion slows down. If the liquid is cooled sufficiently fast, crystallization can be avoided<sup>10,11</sup>. Eventually molecules will rearrange so slowly that they cannot adequately sample configurations in the available time allowed by the cooling rate. The liquid's structure therefore appears 'frozen' on the laboratory timescale (for example, minutes). This falling out of equilibrium occurs across a narrow transformation range where the characteristic molecular relaxation time becomes of the order of 100 seconds, and the rate of change of volume or enthalpy with respect to temperature decreases abruptly (but continuously) to a value comparable to that of a crystalline solid. The resulting material is a glass. The intersection of the liquid and vitreous portions of the volume versus temperature curve provides one definition of  $T_g$ , which usually occurs around  $2T_m/3$ . The behaviour depicted in Fig. 1 is not a true phase transition, as it does not involve discontinuous changes in any physical property.

The slower a liquid is cooled, the longer the time available for configurational sampling at each temperature, and hence the colder it can become before falling out of liquid-state equilibrium. Consequently,  $T_g$  increases with cooling rate<sup>12,13</sup>. The properties of a glass, therefore, depend on the process by which it is formed. In practice, the dependence of  $T_g$  on the cooling rate is weak ( $T_g$  changes by 3–5 °C when the cooling rate changes by an order of magnitude<sup>14</sup>), and the transformation range is narrow, so that  $T_g$  is an important material characteristic.

## Slowing down

Another definition of  $T_g$  is the temperature at which the shear viscosity reaches  $10^{13}$  poise. Close to  $T_g$  the viscosity  $\eta$

is extraordinarily sensitive to temperature. For silica this dependence is reasonably well described by the Arrhenius functionality,  $\eta = A \exp(E/k_B T)$ , where  $A$  and  $E$  are temperature-independent and  $k_B$  is Boltzmann's constant. Other liquids exhibit an even more pronounced viscous slow-down close to the glass transition, which is reasonably well represented, over 2–4 orders of magnitude in viscosity<sup>8</sup>, by the Vogel–Tammann–Fulcher (VTF) equation<sup>15–17</sup>

$$\eta = A \exp[B/(T - T_0)] \quad (1)$$

where  $A$  and  $B$  are temperature-independent constants. Understanding the origin of this extraordinary slow-down of relaxation processes is one of the main challenges in the physics of glasses.

Figure 2 shows a  $T_g$ -scaled Arrhenius representation of liquid viscosities<sup>18–21</sup>. Angell has proposed a useful classification of liquids

along a 'strong' to 'fragile' scale. The viscosity and relaxation times (for example, dielectric relaxation) of the former behave in nearly Arrhenius fashion, whereas fragile liquids show marked deviations from Arrhenius behaviour. Silica ( $\text{SiO}_2$ ) is the prototypical strong liquid, whereas *o*-terphenyl (OTP) is the canonical fragile glass-former. Strong liquids, such as the network oxides  $\text{SiO}_2$  and germanium dioxide ( $\text{GeO}_2$ ), have tetrahedrally coordinated structures, whereas the molecules of fragile liquids exert largely non-directional, dispersive forces on each other. Alternative scaling descriptions that attempt to extract universal aspects of viscous slow-down have been proposed<sup>22–24</sup>. Their relative merits are still being assessed<sup>8,25</sup>.

Viscous liquids close to  $T_g$  exhibit non-exponential relaxation. The temporal behaviour of the response function  $F(t)$  (for example, the polarization in response to an applied electric field, the strain (deformation) resulting from an applied stress, or the stress in

Box 1

Entropy crises

Boltzmann's entropy formula establishes the connection between the microscopic world of atoms and molecules and the bulk properties of matter:

$$S(N, V, E) = k_B \ln \Omega$$

In this equation,  $S$  is the entropy,  $k_B$  is Boltzmann's constant and  $\Omega$  is the number of quantum states accessible to  $N$  particles with fixed energy  $E$  in a volume  $V$ . Because  $\Omega$  cannot be less than one, the entropy cannot be negative. When a crystal is cooled sufficiently slowly, it approaches a unique state of lowest energy, and hence its entropy approaches zero as  $T \rightarrow 0$ . If the entropy of a supercooled liquid were to become smaller than that of the stable crystal at the Kauzmann temperature, its entropy would eventually become negative upon further cooling. This impossible scenario constitutes an entropy crisis<sup>46–48</sup>.

The Kauzmann temperature  $T_K$  is given by<sup>9</sup>

$$\Delta s_m = \int_{T_K}^{T_m} \frac{\Delta C_p}{T} dT$$

where  $\Delta s_m$  is the melting entropy (the difference between liquid and crystal entropies at the melting temperature),  $T_m$  is the melting temperature at the given pressure, and  $\Delta C_p$  is the temperature-dependent difference between the heat capacity of the liquid and the crystal at the given pressure. The rate of change of entropy with temperature at constant pressure is given by

$$\left(\frac{\partial S}{\partial T}\right)_P = \frac{C_p}{T}$$

The entropy crisis arises because the heat capacity of a liquid is greater than that of the stable crystal. The entropy of fusion is therefore consumed upon supercooling, and vanishes at  $T_K$ . The entropy crisis entails no conflict with the second law of thermodynamics, as the difference in chemical potential  $\Delta\mu$  between the supercooled liquid and the stable crystal at  $T_K$  is a positive quantity. Because the chemical potential is the Gibbs free energy per unit mass, this means that the system can reduce its Gibbs free energy by freezing, in accord with experience. The chemical potential difference at  $T_K$  is given by<sup>9</sup>

$$\Delta\mu(T_K) = \int_{T_K}^{T_m} \Delta C_p \left(\frac{T_m}{T} - 1\right) dT$$

One way of avoiding the entropy crisis is for the liquid to form an ideal glass of unique configuration at  $T_K$ . This is the thermodynamic view of the glass transition, according to which the observable glass transition is a manifestation, masked by kinetics, of an underlying second-order phase transition<sup>50</sup> occurring at  $T_K$ .

Because the glass transition intervenes before the entropy crisis occurs ( $T_g > T_K$ ), estimates of the Kauzmann temperature involve an extrapolation of liquid properties below  $T_g$ . The validity of such extrapolations, and hence of the very possibility of an entropy crisis, has been questioned by Stillinger<sup>103</sup>, owing to the apparent necessity for configurational excitations out of the ideal glass state to require an unbounded energy. Furthermore, recent computer simulations of polydisperse hard disks found no evidence of a thermodynamic basis underlying the glass transition<sup>104</sup>. Although the notion of an ideal glass remains controversial<sup>103</sup>, this does not undermine the usefulness of  $T_K$  as an empirical classification parameter for glass-formers.

Experimentally, there are substances with known Kauzmann points. <sup>4</sup>He is a liquid at 0 K and 1 bar (liquid He-II). Its equilibrium freezing pressure at 0 K is 26 bar. At this point, the entropies of the liquid and the crystal are equal, and this is therefore a Kauzmann point, although not an entropy crisis as both phases have zero entropy. The melting curves of <sup>3</sup>He and <sup>4</sup>He exhibit pressure minima: these occur at about 0.32 K and 0.8 K, respectively<sup>105</sup>. These are also equal-entropy (Kauzmann) points. Experiments indicate that poly(4-methylpentene-1) exhibits a pressure maximum along its melting curve<sup>106</sup>. Although the appearance of an additional phase complicates the interpretation of this observation, the implication would be that the pressure maximum is a Kauzmann point, and the continuation of the melting curve to lower temperatures and pressures beyond this point corresponds to endothermic freezing of a stable liquid into a crystal possessing higher entropy<sup>107</sup>. How this liquid would avoid conflict with the third law is not understood, but may hinge on the vibrational anharmonicity of the two phases with changing temperature.

response to an imposed deformation) can often be described by the stretched exponential, or Kohlrausch–Williams–Watts (KWW) function<sup>26,27</sup>

$$F(t) = \exp[-(t/\tau)^\beta] \quad (\beta < 1) \quad (2)$$

where  $F(t) = [\sigma(t) - \sigma(\infty)]/[\sigma(0) - \sigma(\infty)]$  and  $\sigma$  is the measured quantity (for example, the instantaneous stress following a step change in deformation).  $\tau$  in equation (2) is a characteristic relaxation time, whose temperature dependence is often non-Arrhenius (exhibiting fragile behaviour). The slowing down of long-time relaxation embodied in equation (2) contrasts with the behaviour of liquids above the melting point, which is characterized by simple exponential relaxation. Experimental and computational evidence indicates that this slow-down is related to the growth of distinct relaxing domains<sup>28–39</sup> (spatial heterogeneity). Whether each of these spatially heterogeneous domains relaxes exponentially or not is a matter of considerable current interest<sup>38,39</sup>.

### Decouplings

In supercooled liquids below approximately  $1.2T_g$  there occurs a decoupling between translational diffusion and viscosity, and between rotational and translational diffusion<sup>30,39,40</sup>. At higher temperatures, both the translational and the rotational diffusion coefficients are inversely proportional to the viscosity, in agreement with the Stokes–Einstein and Debye equations, respectively. Below approximately  $1.2T_g$ , the inverse relationship between translational motion and viscosity breaks down, whereas that between rotational motion and viscosity does not. Near  $T_g$ , it is found that molecules translate faster than expected based on their viscosity, by as much as two orders of magnitude. This therefore means that, as the temperature is lowered, molecules on average translate progressively more for every rotation they execute. Yet another decoupling occurs in the moderately supercooled range. At sufficiently high temperature the liquid shows a single peak relaxation frequency (Fig. 3), indicative of one relaxation mechanism. In the moderately supercooled regime, however, the peak splits into slow ( $\alpha$ ) and fast ( $\beta$ ) relaxations<sup>41–43</sup>. The former exhibit non-Arrhenius behaviour and disappear at  $T_g$ ; the latter continue below  $T_g$  and display Arrhenius behaviour<sup>44</sup>.

### Thermodynamics

The entropy of a liquid at its melting temperature is higher than that of the corresponding crystal. Because the heat capacity of a liquid is higher than that of the crystal, this entropy difference decreases upon supercooling (Box 1). Figure 4 shows the temperature dependence of the entropy difference between several supercooled liquids and their stable crystals<sup>45</sup>. For lactic acid this entropic surplus is consumed so

fast that a modest extrapolation of experimental data predicts its impending vanishing. In practice, the glass transition intervenes, and  $\Delta S$  does not vanish. If the glass transition did not intervene, the liquid entropy would equal the crystal's entropy at a nonzero temperature  $T_K$  (the Kauzmann temperature.) Because the entropy of the crystal approaches zero as  $T$  tends to zero, the entropy of the liquid would eventually become negative upon cooling if this trend were to continue. Because entropy is an inherently non-negative quantity (Box 1), the state of affairs to which liquids such as lactic acid are tending when the glass transition intervenes is an entropy crisis<sup>46–48</sup>. The extrapolation needed to provoke conflict with the third law is quite modest for many fragile liquids<sup>49</sup>, and the imminent crisis is thwarted by a kinetic phenomenon, the glass transition. This suggests a connection between the kinetics and the thermodynamics of glasses<sup>47</sup>. The thermodynamic viewpoint that emerges from this analysis<sup>50</sup> considers the laboratory glass transition as a kinetically controlled manifestation of an underlying thermodynamic transition to an ideal glass with a unique configuration.

A formula of Adam and Gibbs<sup>51</sup> provides a suggestive connection between kinetics and thermodynamics:

$$t = A \exp(B/Ts_c) \quad (3)$$

In this equation,  $t$  is a relaxation time (or, equivalently, the viscosity) and  $A$  and  $B$  are constants.  $s_c$ , the configurational entropy, is related to the number of minima of the system's multidimensional potential energy surface (Box 2). According to the Adam–Gibbs picture, the origin of viscous slow-down close to  $T_g$  is the decrease in the number of configurations that the system is able to sample. At the Kauzmann temperature the liquid would have attained a unique, non-crystalline state of lowest energy, the ideal glass. Because there is no configurational entropy associated with confinement in such a state, the Adam–Gibbs theory predicts structural arrest to occur at  $T_K$ . In their derivation of equation (3), Adam and Gibbs invoked the concept of a cooperatively rearranging region (CRR)<sup>51</sup>. A weakness of their treatment is the fact that it provides no information on the size of such regions. The fact that the CRRs are indistinguishable from each other is also problematic, in light of the heterogeneity that is believed to underlie stretched exponential behaviour<sup>8</sup>.

**Figure 1** Temperature dependence of a liquid's volume  $v$  or enthalpy  $h$  at constant pressure.  $T_m$  is the melting temperature.

A slow cooling rate produces a glass transition at  $T_{ga}$ ; a faster cooling rate leads to a glass transition at  $T_{gb}$ . The thermal expansion coefficient  $\alpha_p = (\partial \ln v / \partial T)_p$  and the isobaric heat capacity  $c_p = (\partial h / \partial T)_p$  change abruptly but continuously at  $T_g$ .

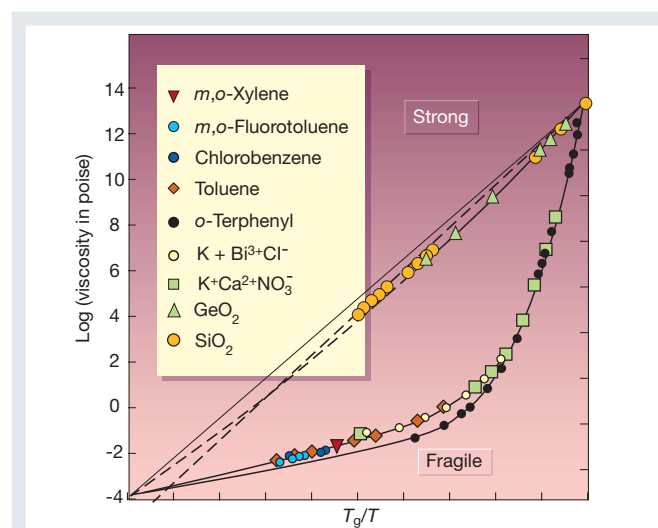
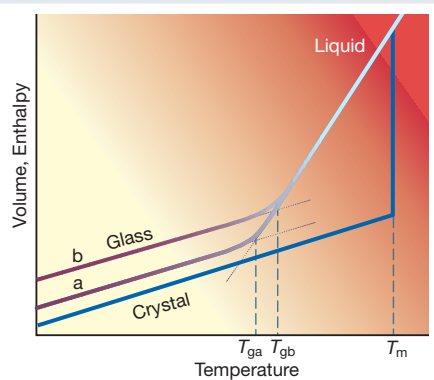


**Figure 2**  $T_g$ -scaled Arrhenius representation of liquid viscosities showing Angell's strong–fragile pattern. Strong liquids exhibit approximate linearity (Arrhenius behaviour), indicative of a temperature-independent activation energy  $E = d \ln \eta / d(1/T) \approx \text{const}$ . Fragile liquids exhibit super-Arrhenius behaviour, their effective activation energy increasing as temperature decreases. (Adapted from refs 9 and 11.)

Nevertheless, equation (3) describes the relaxation behaviour of deeply supercooled liquids remarkably well. If the difference in heat capacities between a supercooled liquid and its stable crystalline form is inversely proportional to temperature<sup>52</sup>, the Adam–Gibbs

relation yields the VTF equation, which is mathematically equivalent to the Williams–Landel–Ferry equation for the temperature dependence of viscosity in polymers<sup>53</sup>. This transformation is predicated on the assumption that the vibrational entropies of the

Box 2

Statistics of landscapes

The complexity of many-body landscapes makes a statistical description inevitable. The quantity of interest is the number of minima of given depth, which is given by<sup>108</sup>

$$\frac{d\Omega}{d\phi} = C \exp[N\sigma(\phi)]$$

Here,  $d\Omega$  denotes the number of potential energy minima with depth per particle ( $\phi = \Phi/N$ ) between  $\phi$  and  $\phi \pm d\phi/2$ .  $C$  is an  $N$ -independent factor with units of inverse energy, and  $\sigma(\phi)$ , also an  $N$ -independent quantity, is a so-called basin enumeration function. Taking the logarithm of the above expression and comparing with Boltzmann's entropy formula (Box 1), we see that  $\sigma(\phi)$  is the entropy per particle arising from the existence of multiple minima of depth  $\phi$ , or, in other words, the configurational entropy.

At low temperatures, it is possible to separate the configurational contribution to thermophysical properties, which arises from the exploration of different basins, from the vibrational component, which arises from thermal motions confined to a given basin<sup>75,76</sup>. The Helmholtz free energy  $A$  is then given by

$$\frac{A}{NkT} = \frac{\bar{\phi}}{kT} - \sigma(\bar{\phi}) + \frac{a^v}{k_B T}$$

where  $\bar{\phi}$  is the depth of the basins preferentially sampled at the given temperature, and  $a^v$  is the vibrational free energy per particle. Thus, the free energy consists of an energetic component that reflects the depth of landscape basins sampled preferentially at the given temperature, an entropic component that accounts for the number of existing basins of a given depth, and a vibrational component. The statistical description of a landscape consists of the basin enumeration function  $\sigma(\phi)$ , from which the excitation profile  $\phi(T)$  is obtained through the free-energy minimization condition

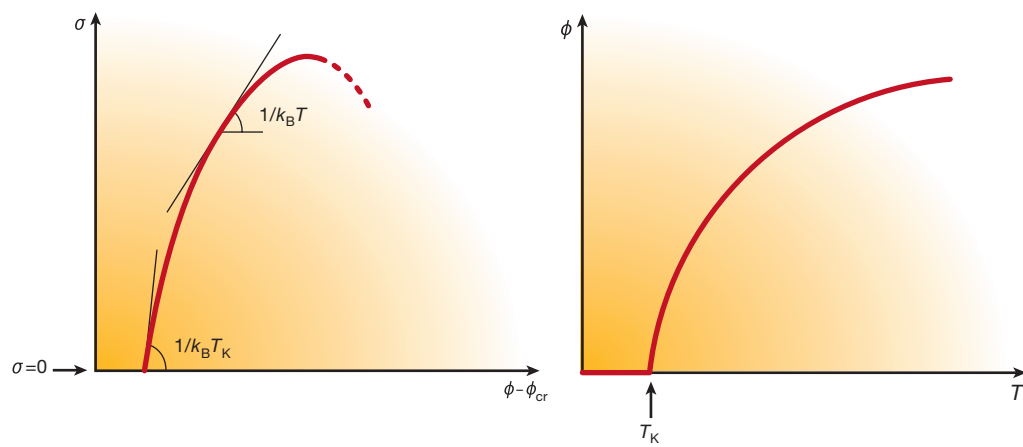
$$\frac{d\sigma}{d\phi} = \frac{1}{k_B T}$$

The above equation assumes that  $a^v$  depends on  $T$ , but not on  $\phi$  — that is, all basins have the same mean curvature at their respective minima.

The shape of a given system's landscape is determined by the density (number of molecules per unit volume,  $N/V$ ). Temperature governs the manner in which the landscape is sampled. A different basin enumeration function and excitation profile corresponds to each density. Temperature dictates the point along the enumeration curve and the excitation profile sampled by the system at fixed density (see figure below).

It is possible to construct the basin enumeration function and excitation profile of a system from experimental heat capacity data for the crystal and the supercooled liquid<sup>109</sup>, and by computer simulation<sup>77,78</sup>. In the latter case, the calculations involve determining the probability distribution of inherent structure energies sampled as a function of temperature. These calculations are at the limit of what is presently feasible with available computational power. The enumeration function is often well represented by a parabola, indicative of a gaussian distribution of basins<sup>4,77,97</sup>. At present it is not understood how the enumeration function deforms with density for a given system (but see ref. 96 for a recent example of such a calculation), or how it depends on molecular architecture. Understanding such questions would provide a direct link between landscape statistics and physical properties. The success of the Adam–Gibbs equation indicates that this link applies also to transport properties such as diffusion and viscosity.

**Box 2 Figure** Schematic representation of the basin enumeration function (left) and the excitation profile (right).  $\phi$  is the potential energy per particle in mechanically stable potential energy minima.  $\phi_{cr}$  is the corresponding quantity in the stable crystal. The number of potential energy minima with depth between  $\phi$  and  $\phi \pm d\phi/2$  is proportional to  $\exp[N\sigma(\phi)]$ . In the thermodynamic limit ( $N$  of the order of Avogadro's number,  $6.02 \times 10^{23}$ ), basins that possess larger (less negative) potential energies (shallow basins) are overwhelmingly more numerous than deeper basins possessing very negative  $\phi$ -values. The slope of the enumeration function is inversely proportional to the temperature. The excitation profile gives the depth of the inherent structures sampled preferentially at a given temperature. At the Kauzmann temperature  $T_K$  the system attains the state of a configurationally unique ideal glass ( $\sigma=0$ ), corresponding to the deepest amorphous basin (see Figs 5 and 8) and its inherent structure energy does not therefore change upon further cooling.





supercooled liquid and its stable crystal are equal<sup>9</sup>. For many fragile glass-formers the VTF temperature of structural arrest,  $T_o$ , is very close to  $T_K$  obtained from calorimetric measurements (typically<sup>49</sup>  $0.9 < T_K/T_o < 1.1$ ). This again indicates a connection between dynamics and thermodynamics not present at higher temperatures. Equally suggestive is the correspondence between kinetic fragilities based on the temperature dependence of the viscosity (see Fig. 2) and thermodynamic fragilities<sup>54</sup>, based on the temperature dependence of the entropy surplus of the supercooled liquid with respect to its stable crystal.

### The energy landscape

A convenient framework for interpreting the complex phenomenology just described is provided by the energy landscape<sup>44</sup>. This is the name generally given to the potential energy function of an  $N$ -body system  $\Phi(r_1, \dots, r_N)$ , where the vectors  $r_i$  comprise position, orientation and vibration coordinates. In condensed phases, whether liquid or solid, every molecule experiences simultaneous interactions with numerous neighbours. Under these conditions it is convenient to consider the full  $N$ -body  $\Phi$ -function. The landscape is a multidimensional surface. For the simplest case of  $N$  structureless particles possessing no internal orientational and vibrational degrees of freedom, the landscape is a  $(3N + 1)$ -dimensional object. Figure 5 is a schematic illustration of an energy landscape. The quantities of interest are the number of potential energy minima (also called inherent structures) of a given depth (Box 2), and the nature of the saddle points separating neighbouring minima. More than 30 years ago, Goldstein articulated a topographic viewpoint of condensed phases<sup>55</sup> that has come to be known as the energy landscape paradigm. His seminal ideas have since been applied to protein folding<sup>56–64</sup>, the mechanical properties of glasses<sup>65–67</sup>, shear-enhanced diffusion<sup>68</sup> and the dynamics of supercooled liquids<sup>69–71</sup>.

### Landscape sampling

For an  $N$ -body material system in a volume  $V$ , the landscape is fixed. The manner in which a material system samples its landscape as a

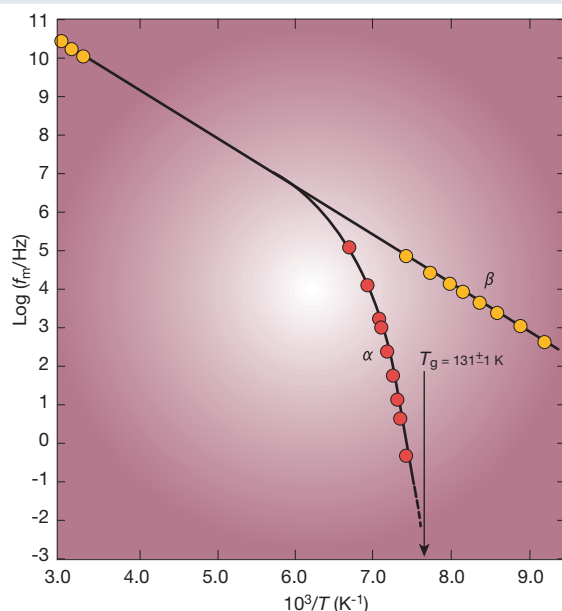


**Figure 3** Temperature dependence of the peak dielectric relaxation frequency of the glass-forming mixture chlorobenzene/*cis*-decalin (molar ratio 17.2/82.8%). At high enough temperature there is a single relaxation mechanism. In the moderately supercooled regime the peak splits into slow ( $\alpha$ ) and fast ( $\beta$ ) relaxations, of which  $\alpha$ -processes exhibit non-Arrhenius temperature dependence and vanish at  $T_g$ . (Adapted from refs 9 and 41.)

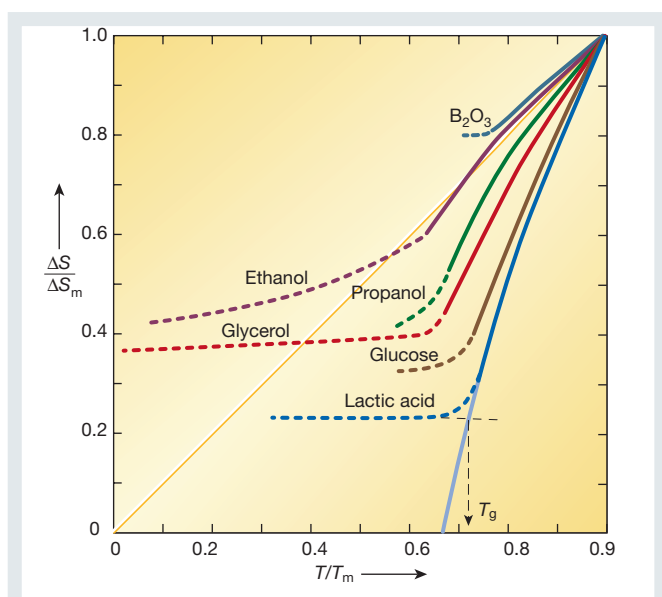


**Figure 4** Temperature dependence of the entropy difference between several supercooled liquids and their stable crystals at atmospheric pressure.  $\Delta S_m$  is the melting entropy and  $T_m$  is the melting temperature. The glass transition always intervenes before the vanishing of the entropy surplus. For fragile liquids such as lactic acid, however, an entropy crisis is imminent. (Adapted from ref. 45.)

function of temperature provides information on its dynamic behaviour<sup>70</sup>. The way that a landscape deforms as a result of changes in density provides information on the mechanical properties of a material system<sup>72</sup>. Figure 6 shows the average inherent structure energy for a mixture of unequal-sized atoms, as a function of the temperature of the equilibrated liquid<sup>70,73</sup>. In these calculations, molecular dynamics simulations of the binary mixture were performed to generate configurations. Periodically, the system's energy was minimized, yielding mechanically stable inherent structures, the average energy of which is reported in the figure. At high temperatures the inherent structure energy is virtually temperature-independent, and appears to have reached a plateau. When the system has sufficient kinetic energy to sample its entire energy landscape, the overwhelming number of minima that it samples are shallow, reflecting the fact that deep minima are very rare (Box 2). But as the reduced temperature decreases below about  $T = 1$ , the system is unable to surmount the highest energy barriers, and is therefore forced to sample the much rarer deeper minima (Box 2). When this happens, the kinetics of structural relaxation changes from exponential to stretched exponential, and the activation energy (and entropy) associated with structural relaxation become super-Arrhenius, that is to say they increase with decreasing temperature<sup>70</sup>.

These calculations established a connection between changes in dynamics and the manner in which the static and thermodynamic energy landscape is sampled as a function of temperature. Figure 6 also shows that at a low enough temperature the system becomes stuck in a single minimum, the depth of which increases as the cooling rate decreases. This corresponds to the glass transition. Another important observation of this study was the existence of a temperature  $T \approx 0.45$ , below which the height of the barriers separating sampled inherent structures increases abruptly. This temperature was found to correspond closely to the crossover temperature predicted by mode-coupling theory (MCT; see below) for this system. Here again, it is the manner in which the system samples its landscape, not the landscape itself, that changes with temperature. (See ref. 74 for a recent, different interpretation of landscape sampling at this temperature.)

The landscape picture provides a natural separation of low-temperature molecular motion into sampling distinct potential

energy minima, and vibration within a minimum. It is possible to separate formally the corresponding configurational and vibrational contributions to a liquid's properties<sup>75,76</sup>. In two important computational studies, the configurational entropy was calculated by probing systematically the statistics governing the sampling of potential energy minima<sup>77,78</sup> (Box 2). Using this technique, a remarkable connection between configurational entropy and diffusion was identified in liquid water<sup>79</sup>. One of water's distinguishing anomalies is the fact that, at sufficiently low temperature, its diffusivity increases upon compression<sup>80</sup>. As shown in Fig. 7, diffusivity maxima are correlated strongly with configurational entropy maxima, the respective loci coinciding within numerical error.

The results shown in Fig. 7 and the success of the Adam–Gibbs equation in describing experimental data on relaxation in a wide variety of systems<sup>52</sup> indicate that there exists a scaling relationship between the depth distribution of basins and the height of the saddle points along paths connecting neighbouring basins. Such scaling is not a mathematical necessity, but arises from the nature of real molecular interactions. The topographic nature of this statistical scaling relationship between minima and saddle points is poorly understood (but see the recent computational investigation of saddle points<sup>74</sup>). Its elucidation will explain the origin of the connection between the dynamics and thermodynamics of glass-forming liquids, and constitutes the principal theoretical challenge in this field.

**Strong versus fragile behaviour**

The extent to which the shear viscosity  $\eta$  deviates from Arrhenius behaviour,  $\eta = \eta_0 \exp(E/k_B T)$ , constitutes the basis of the classification of liquids as either strong or fragile (Fig. 2). Molten SiO<sub>2</sub>, often considered as the prototypical strong glass-former, displays an almost constant activation energy of 180 kcal mol<sup>-1</sup> (ref. 81). This constancy indicates that the underlying mechanism, presumably breaking and reformation of Si–O bonds, applies throughout the entire landscape<sup>4</sup>. In contrast, the viscosity of OTP — the canonical fragile glass-former — deviates markedly from Arrhenius behaviour<sup>82</sup>, showing an effective activation energy (dln  $\eta$ /d1/T) that increases 20-fold, from one-quarter of the heat of vaporization for the liquid above its melting point to roughly five times the heat of vaporization near  $T_g$ . This means that OTP's landscape is very heterogeneous. The basins sampled at high temperature allow relaxation by surmounting low barriers involving the rearrangement of a small number of molecules. The very large activation energy at  $T \approx T_g$ , on the other hand, corresponds to the cooperative rearrangement of many molecules. These differences between strong and fragile behaviour imply a corresponding topographic distinction between the two

archetypal landscapes. Aside from multiplicity due to permutational symmetry, strong landscapes may consist of a single 'megabasin', whereas fragile ones display a proliferation of well-separated 'megabasins' (Fig. 8).

Cooperative rearrangements such as those that must occur in OTP are unlikely to consist of elementary transitions between adjacent basins. Rather, the likely scenario involves a complicated sequence of elementary transitions. At low temperatures, these rearrangements should be rare and long-lived on the molecular timescale. Furthermore, the diversity of deep landscape traps and of the pathways of configuration space that connect them should result in a broad spectrum of relaxation times, as required for the stretched exponential function in equation (2). This in turn suggests that supercooled fragile liquids are dynamically heterogeneous, probably consisting at any instant of mostly non-diffusing molecules with a few 'hot spots' of mobile molecules. This dynamic heterogeneity<sup>39</sup> has both experimental<sup>29,30,36</sup> and computational<sup>31–35</sup> support.

The inverse relation between the self-diffusion coefficient and viscosity embodied in the Stokes–Einstein equation is based on macroscopic hydrodynamics that treats the liquid as a continuum.

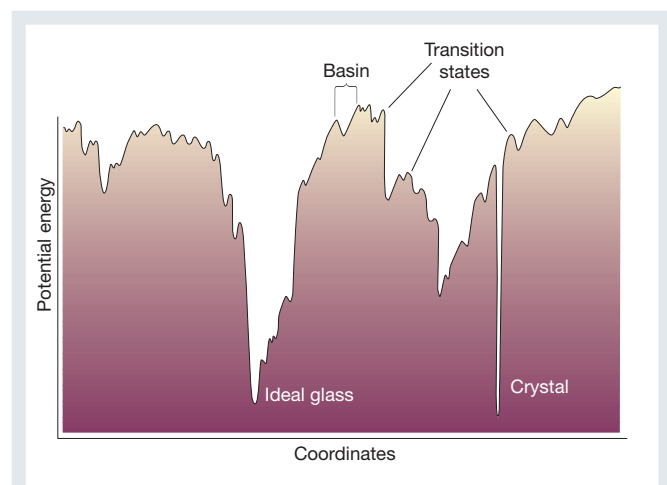


**Figure 5** Schematic illustration of an energy landscape. The x-axis represents all configurational coordinates. (Adapted from ref. 44.)

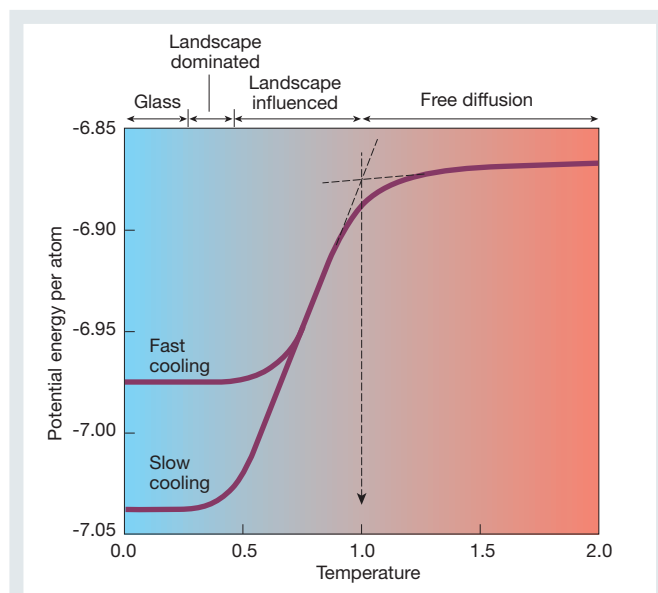


**Figure 6** Mean inherent structure energy per particle of a binary mixture of unequal-sized Lennard–Jones atoms, as a function of the temperature of the equilibrated liquid from which the inherent structures were generated by energy minimization. Molecular dynamics simulations at constant energy and density were performed over a range of temperatures for 256 Lennard–Jones atoms, of which 20% are of type A and 80% are of type B. The Lennard–Jones size and energy parameters are  $\sigma_{AA} = 1$ ,  $\sigma_{BB} = 0.88$ ,  $\sigma_{AB} = 0.8$ , and  $\epsilon_{AA} = 1$ ,  $\epsilon_{BB} = 0.5$ ,  $\epsilon_{AB} = 1.5$ , respectively. Length, temperature, energy and time are expressed in units of  $\sigma_{AA}$ ,  $\epsilon_{AA}/k_B$ ,  $\epsilon_{AA}$  and  $\sigma_{AA}(m/\epsilon_{AA})^{1/2}$ , respectively, with  $m$  representing the mass of the particles. Simulations were performed at a density of 1.2. The fast and slow cooling rates are  $1.08 \times 10^{-3}$  and  $3.33 \times 10^{-6}$ . When  $T > 1$ , the system has sufficient kinetic energy to sample the entire energy landscape, and the overwhelming number of sampled energy minima are shallow. Under these conditions, the system exhibits a temperature-independent activation energy for structural relaxation (calculations not shown). Between  $T = 1$  and  $T \approx 0.45$ , the activation energy increases upon cooling, the dynamics become 'landscape-influenced', and the mechanically stable configurations sampled are strongly temperature-dependent. Below  $T \approx 0.45$ , the height of the barriers separating sampled adjacent energy minima seems to increase abruptly (calculations not shown). This is the 'landscape-dominated' regime. In it, particles execute rare jumps over distances roughly equal to interparticle separations. The crossover between landscape-influenced and landscape-dominated behaviour corresponds closely with the mode-coupling transition temperature<sup>70,92</sup>. (Adapted from refs 70 and 72.)

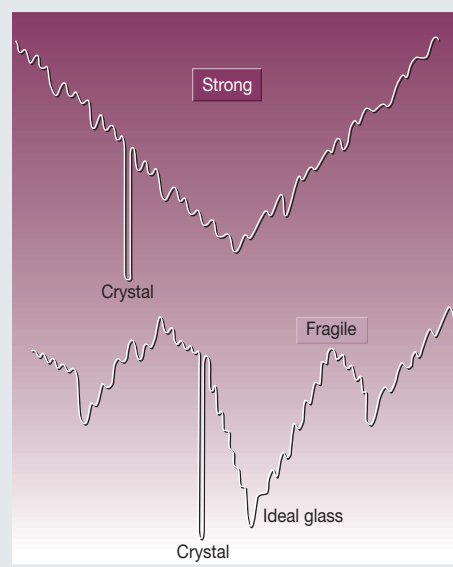
This picture must clearly break down in supercooled fragile liquids, which are dynamically heterogeneous. The failure of the Stokes–Einstein equation, referred to above as one of the distinguishing characteristics of fragile supercooled liquids, is therefore qualitatively understandable. Plausible models for the low-temperature enhancement of diffusive motion relative to hydrodynamic expectations based on the viscosity have been proposed<sup>83–85</sup>, but an accurate predictive theory is missing. The landscape viewpoint also provides a plausible interpretation for the  $\alpha/\beta$ -relaxation decoupling shown in Fig. 3 —  $\alpha$ -relaxations correspond to configurational sampling of neighbouring megabasins (Fig. 8), whereas  $\beta$ -processes are thought to correspond to elementary relaxations between contiguous basins<sup>44</sup>. Direct computational evidence of this interpretation is not available.

### Avoided singularities

Alternative viewpoints to the landscape perspective have also contributed to current understanding of some aspects of supercooling and the glass transition. Two such interpretations invoke a narrowly avoided singularity above  $T_g$ .

According to MCT<sup>86</sup>, structural arrest occurs as a result of the following feedback mechanism: (i) shear-stress relaxation occurs primarily through diffusive motion; (ii) diffusion and viscosity are inversely related; and (iii) viscosity is proportional to shear-stress relaxation time. These facts lead to a viscosity feedback whereby

**Figure 8** Schematic representation of the energy landscapes of strong and fragile substances. The potential energy increases vertically, and the horizontal direction represents collective configurational coordinates.



structural arrest occurs as a purely dynamic singularity, that is to say it is not accompanied by thermodynamic signatures such as a diverging correlation length. What is now known as the idealized MCT<sup>87,88</sup> predicts structural arrest to occur at a temperature  $T_x$ . Initially, therefore, it was thought that MCT was a useful theory for the laboratory-generated glass transition. It is now widely understood that this is not the case, as one finds that  $T_x > T_g$ , and the MCT-predicted singularity does not occur. In subsequent modifications of the theory<sup>89</sup>, additional relaxation mechanisms occur, often referred to as ‘hopping’ or activated motions, which restore ergodicity (the system’s ability to sample all configurations) below  $T_x$ , thereby avoiding a kinetic singularity. These additional relaxation modes arise as a result of a coupling between fluctuations in density and momentum.

Although not a theory of the glass transition, MCT accurately describes many important aspects of relaxation dynamics in liquids above or moderately below their melting temperatures. In particular, the theory makes detailed predictions about the behaviour of the intermediate scattering function  $F$ , an experimentally observable quantity that measures the decay of density fluctuations. After a fast initial decay due to microscopic intermolecular collisions, MCT predicts that the decay of  $F$  obeys the following sequence (Fig. 9): (i) power-law decay towards a plateau, according to  $F = f + At^{-a}$ ; (ii) a second power-law decay away from the plateau value  $F = f - Bt^b$ ; and (iii) slow relaxation at longer times, which can be fitted by the KWW function  $F = \exp[-(t/\tau)^\beta]$ . Here,  $f$  is the plateau value of the scattering function, which only appears at sufficiently low temperature;  $t$  is time;  $A$ ,  $B$ ,  $a$  and  $b$  are constants;  $\tau$  is the characteristic, temperature-dependent relaxation time; and  $\beta < 1$  is the KWW stretch exponent. The basic accuracy of these detailed predictions has been verified experimentally and in computer simulations<sup>90–92</sup>.

Kivelson and co-workers have proposed a theory of supercooled liquids that is based also on an avoided singularity<sup>24,93–95</sup>. According to this viewpoint, the liquid has an energetically preferred local structure that differs from the structure in the actual crystalline phase. The system is prevented from crystallizing into a reference crystal with the preferred local structure because of geometric frustration owing to the fact that the latter does not tile space. An example of such energetically favoured but non-space-tiling local structure is the icosahedral packing seen in computer simulations of the supercooled Lennard–Jones liquid<sup>73</sup>. At a temperature  $T^*$  the system would, but for frustration, crystallize into the reference crystal. Instead, strain build-up causes the system to break up into frustration-limited domains, thereby avoiding a phase transition (singularity) at  $T^*$ . The avoided transition temperature  $T^*$  acts as a critical point, below which two length scales emerge, both of which are large compared to

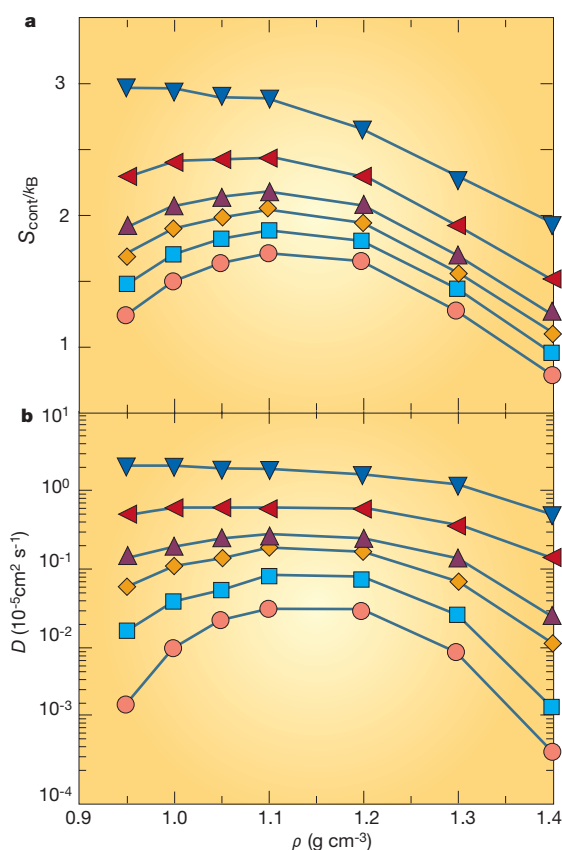


**Figure 7** Relationship between diffusivity ( $D$ ) and configurational entropy ( $S_{\text{conf}}$ ) of supercooled water<sup>79</sup> at six different temperatures. Filled and open symbols from top to bottom represent the following temperatures: 300 K, 260 K, 240 K, 230 K, 220 K and 210 K;  $\rho$  is density. The configurational entropy, which is related to the number of potential energy minima of a given depth (Box 2), was calculated by subtracting the vibrational contribution from the total entropy. The calculations involved performing molecular dynamics simulations of the extended simple point charge (SPC/E) model of water<sup>102</sup> over a range of temperatures and densities. (Adapted from ref. 79.)



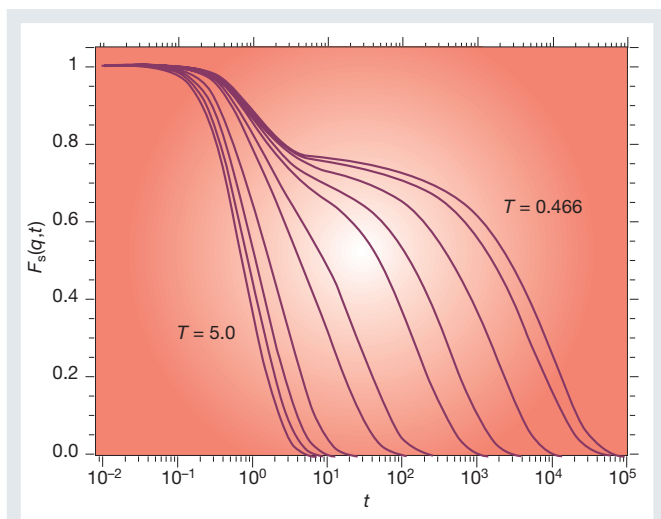


**Figure 9** Evolution of the self-intermediate scattering function for A-type atoms for the same supercooled Lennard–Jones mixture as in Fig. 6, at  $q\sigma_{AA} = 7.251$ , corresponding to the first peak of the static structure factor of species A (ref. 92). Here  $q$  is the magnitude of the wave vector. Temperature and time are in units of  $\epsilon_{AA}/k_B$  and  $\sigma_{AA}(m/48\epsilon_{AA})^{1/2}$ , respectively. Temperatures from left to right are 5, 4, 3, 2, 1, 0.8, 0.6, 0.55, 0.5, 0.475, and 0.466. The self-intermediate scattering function is the space Fourier transform of the van Hove function  $G_s(r, t)$ , which is proportional to the probability of observing a particle at  $r \pm dr$  at time  $t$  given that the same particle was at the origin at  $t = 0$ . Note the two-step relaxation behaviour upon decreasing  $T$ . Molecular dynamics simulations of 1,000 atoms. (Adapted from refs 9 and 92.)

molecular dimensions. One is the critical correlation length, which governs density fluctuations in the absence of frustration. The second is the frustration-limited domain size. From these considerations there emerge predictions on the temperature dependence of the viscosity. Experimental data analysed according to the theory display universality<sup>24</sup>, but at the expense of introducing a number of fitting parameters. The improvement with respect to competing interpretations is a matter of controversy<sup>25</sup>.

### Challenges and open questions

Important aspects of the complex behaviour of viscous liquids close to the glass transition can be explained qualitatively from the energy landscape perspective. Making this descriptive picture quantitative and predictive is a major challenge. This will require investigating how basic landscape features such as the basin enumeration function depend on molecular architecture and, for a given substance or mixture, on density (see ref. 96 for an example of such a calculation). Equally important is the translation of qualitative pictures such as Fig. 8 into precise measures of strength and fragility based on the basin enumeration function. Uncovering the topographic nature of the scaling relationship between basin minima and saddle points holds the key to understanding the relationship between kinetics and thermodynamics in deeply supercooled liquids. All of these calculations are in principle straightforward, but computationally at the very limit of what is currently feasible. The development of theoretical models<sup>97</sup> is therefore of paramount importance.

MCT and the landscape perspective offer complementary viewpoints of the same phenomena. So far, however, not enough effort has been devoted to bridging the gap that separates these two approaches. Recent calculations<sup>70,74</sup> offer the promise of establishing a clearer connection between the static landscape viewpoint and the dynamic perspective of MCT. At the least, what is required is a precise landscape-based explanation of what ‘hopping’ and ‘activated processes’ really mean. Additional theoretical viewpoints of supercooling and the glass transition include the instantaneous normal-mode perspective on liquid dynamics<sup>98</sup> and thermodynamic

treatments of the vitreous state based on invoking analogies to spin glasses<sup>99–101</sup>. Establishing a coherent theoretical perspective on supercooled liquids and glasses is important. We believe that the landscape formalism offers the natural technical tools for accomplishing this task. □

1. Angell, C. A. Formation of glasses from liquids and biopolymers. *Science* **267**, 1924–1935 (1995).
2. Blanshard, J. M. V. & Lillford, P. (eds) *The Glassy State in Foods* (Nottingham Univ. Press, Nottingham, 1993).
3. Crowe, J. H., Carpenter, J. F. & Crowe, L. M. The role of vitrification in anhydrobiosis. *Annu. Rev. Physiol.* **60**, 73–103 (1998).
4. Debenedetti, P. G., Stillinger, F. H., Truskett, T. M. & Lewis, C. P. Theory of supercooled liquids and glasses: energy landscape and statistical geometry perspectives. *Adv. Chem. Eng.* (in the press).
5. Greer, A. L. Metallic glasses. *Science* **267**, 1947–1953 (1995).
6. Jenniskens, P. & Blake, D. F. Structural transitions in amorphous water ice and astrophysical implications. *Science* **265**, 753–756 (1994).
7. Anderson, P. W. Through a glass lightly. *Science* **267**, 1615 (1995).
8. Angell, C. A., Ngai, K. L., McKenna, G. B., McMillan, P. F. & Martin, S. W. Relaxation in glass-forming liquids and amorphous solids. *J. Appl. Phys.* **88**, 3113–3157 (2000).
9. Debenedetti, P. G. *Metastable Liquids. Concepts and Principles* (Princeton Univ. Press, Princeton, 1996).
10. Turnbull, D. Under what conditions can a glass be formed? *Contemp. Phys.* **10**, 473–488 (1969).
11. Angell, C. A. Structural instability and relaxation in liquid and glassy phases near the fragile liquid limit. *J. Non-Cryst. Solids* **102**, 205–221 (1988).
12. Moynihan, C. T. et al. in *The Glass Transition and the Nature of the Glassy State* (eds Goldstein, M. & Simha, R.) *Ann. NY Acad. Sci.* **279**, 15–36 (1976).
13. Brüning, R. & Samwer, K. Glass transition on long time scales. *Phys. Rev. B* **46**, 318–322 (1992).
14. Ediger, M. D., Angell, C. A. & Nagel, S. R. Supercooled liquids and glasses. *J. Phys. Chem.* **100**, 13200–13212 (1996).
15. Vogel, H. Das temperatur-abhängigkeitsgesetz der viskosität von flüssigkeiten. *Phys. Zeit.* **22**, 645–646 (1921).
16. Tamman, G. & Hesse, W. Die abhängigkeit der viskosität von der temperatur bei unterkühlten flüssigkeiten. *Z. Anorg. Allg. Chem.* **156**, 245–257 (1926).
17. Fulcher, G. S. Analysis of recent measurements of the viscosity of glasses. *J. Am. Ceram. Soc.* **8**, 339 (1925).
18. Laughlin, W. T. & Uhlmann, D. R. Viscous flow in simple organic liquids. *J. Phys. Chem.* **76**, 2317–2325 (1972).
19. Angell, C. A. in *Relaxations in Complex Systems* (eds Ngai, K. & Wright, G. B.) 1 (Nat'l Technol. Inform. Ser., US Dept. of Commerce, Springfield, VA, 1985).
20. Angell, C. A. Relaxation in liquids, polymers and plastic crystals—strong/fragile patterns and problems. *J. Non-Cryst. Solids* **131–133**, 13–31 (1991).
21. Green, J. L., Ito, K., Xu, K. & Angell, C. A. Fragility in liquids and polymers: new, simple quantifications and interpretations. *J. Phys. Chem. B* **103**, 3991–3996 (1999).
22. Novikov, V. N., Rössler, E., Malinovsky, V. K. & Surovstev, N. V. Strong and fragile liquids in percolation approach to the glass transition. *Europhys. Lett.* **35**, 289–294 (1996).
23. Fujimori, H. & Oguni, M. Correlation index  $(T_{\infty} - T_{\infty})/T_{\infty}$  and activation energy ratio  $\Delta E_{\infty}/\Delta E_{\infty}$  as parameters characterizing the structure of liquid and glass. *Solid State Commun.* **94**, 157–162 (1995).
24. Kivelson, D., Tarjus, G., Zhao, X. & Kivelson, S. A. Fitting of viscosity: distinguishing the temperature dependencies predicted by various models of supercooled liquids. *Phys. Rev. E* **53**, 751–758 (1996).
25. Cummins, H. Z. Comment on ‘‘Fitting of viscosity: distinguishing the temperature dependencies predicted by various models of supercooled liquids’’. *Phys. Rev. E* **54**, 5870–5872 (1996).
26. Kohlrausch, R. Theorie des elektrischen rückstandes in der leidener flasche. *Ann. Phys. Chem. (Leipzig)* **91**, 179–214 (1874).
27. Williams, G. & Watts, D. C. Non-symmetrical dielectric relaxation behavior arising from a simple empirical decay function. *Trans. Faraday Soc.* **66**, 80–85 (1970).
28. Richert, R. & Blumen, A. in *Disorder Effects on Relaxational Processes* (eds Richert, R. & Blumen, A.) 1–7 (Springer, Berlin, 1994).
29. Cicerone, M. T. & Ediger, M. D. Relaxation of spatially heterogeneous dynamic domains in supercooled ortho-terphenyl. *J. Chem. Phys.* **103**, 5684–5692 (1995).
30. Cicerone, M. T. & Ediger, M. D. Enhanced translation of probe molecules in supercooled o-terphenyl: signature of spatially heterogeneous dynamics? *J. Chem. Phys.* **104**, 7210–7218 (1996).
31. Mel’cuk, A. I., Ramos, R. A., Gould, H., Klein, W. & Mountain, R. D. Long-lived structures in fragile glass-forming liquids. *Phys. Rev. Lett.* **75**, 2522–2525 (1995).
32. Hurley, M. M. & Harrowell, P. Non-gaussian behavior and the dynamical complexity of particle motion in a dense two-dimensional liquid. *J. Chem. Phys.* **105**, 10521–10526 (1996).
33. Perera, D. N. & Harrowell, P. Measuring diffusion in supercooled liquids: the effect of kinetic inhomogeneities. *J. Chem. Phys.* **104**, 2369–2375 (1996).
34. Perera, D. N. & Harrowell, P. Consequence of kinetic inhomogeneities in glasses. *Phys. Rev. E* **54**, 1652–1662 (1996).
35. Donati, C., Glotzer, S. C., Poole, P. H., Kob, W. & Plimpton, S. J. Spatial correlations of mobility and immobility in a glass-forming Lennard–Jones liquid. *Phys. Rev. E* **60**, 3107–3119 (1999).
36. Böhrer, R., Hinze, G., Diezemann, G., Geil, B. & Sillescu, H. Dynamic heterogeneity on supercooled ortho-terphenyl studied by multidimensional deuteron NMR. *Europhys. Lett.* **36**, 55–60 (1996).
37. Wang, C.-Y. & Ediger, M. D. How long do regions of different dynamics persist in supercooled o-terphenyl? *J. Phys. Chem. B* **103**, 4177–4184 (1999).
38. Vidal Russell, E. & Israeloff, N. E. Direct observation of molecular cooperativity near the glass transition. *Nature* **408**, 695–698 (2000).
39. Ediger, M. D. Spatially heterogeneous dynamics in supercooled liquids. *Annu. Rev. Phys. Chem.* **51**, 99–128 (2000).
40. Fujara, F., Geil, B., Sillescu, H. H. & Fleischer, G. Translational and rotational diffusion in supercooled ortho-terphenyl close to the glass transition. *Z. Phys. B Cond. Matt.* **88**, 195–204 (1992).
41. Johari, G. P. Intrinsic mobility of molecular glasses. *J. Chem. Phys.* **58**, 1766–1770 (1973).
42. Johari, G. P. & Goldstein, M. Viscous liquids and the glass transition. II. Secondary relaxations in glasses of rigid molecules. *J. Chem. Phys.* **53**, 2372–2388 (1970).



43. Rössler, E., Warschewske, U., Eiermann, P., Sokolov, A. P. & Quitmann, D. Indications for a change of transport mechanism in supercooled liquids and the dynamics close and below  $T_g$ . *J. Non-Cryst. Solids* **172–174**, 113–125 (1994).
44. Stillinger, F. H. A topographic view of supercooled liquids and glass formation. *Science* **267**, 1935–1939 (1995).
45. Kauzmann, W. The nature of the glassy state and the behavior of liquids at low temperatures. *Chem. Rev.* **43**, 219–256 (1948).
46. Simon, F. Über den Zustand der unterkühlten Flüssigkeiten und Gläser. *Z. Anorg. Allg. Chem.* **203**, 219–227 (1931).
47. Wolynes, P. G. Aperiodic crystals: biology, chemistry and physics in a fugue with stretto. *AIP Conf. Proc.* **180**, 39–65 (1988).
48. Wolynes, P. G. Entropy crises in glasses and random heteropolymers. *J. Res. Natl. Inst. Standards Technol.* **102**, 187–194 (1997).
49. Angell, C. A. Landscapes with megabasins: polyamorphism in liquids and biopolymers and the role of nucleation in folding and folding diseases. *Physica D* **107**, 122–142 (1997).
50. Gibbs, J. H. & DiMarzio, E. A. Nature of the glass transition and the glassy state. *J. Chem. Phys.* **28**, 373–383 (1958).
51. Adam, G. & Gibbs, J. H. On the temperature dependence of cooperative relaxation properties in glass-forming liquids. *J. Chem. Phys.* **43**, 139–146 (1965).
52. Richert, R. & Angell, C. A. Dynamics of glass-forming liquids. V. On the link between molecular dynamics and configurational entropy. *J. Chem. Phys.* **108**, 9016–9026 (1998).
53. Williams, M. L., Landel, R. F. & Ferry, J. D. The temperature dependence of the relaxation mechanisms in amorphous polymers and other glass-forming liquids. *J. Am. Chem. Soc.* **77**, 3701–3707 (1955).
54. Ito, K., Moynihan, C. T. & Angell, C. A. Thermodynamic determination of fragility in liquids and a fragile-to-strong liquid transition in water. *Nature* **398**, 492–495 (1999).
55. Goldstein, M. Viscous liquids and the glass transition: a potential energy barrier picture. *J. Chem. Phys.* **51**, 3728–3739 (1969).
56. Frauenfelder, H., Sligar, S. G. & Wolynes, P. G. The energy landscapes and motions of proteins. *Science* **254**, 1598–1603 (1991).
57. Nienhaus, G. U., Müller, J. D., McMahon, B. H. & Frauenfelder, H. Exploring the conformational energy landscape of proteins. *Physica D* **107**, 297–311 (1997).
58. Abkevich, V. I., Gutin, A. M. & Shakhnovich, E. I. Free energy landscape for protein folding kinetics: intermediates, traps, and multiple pathways in theory and lattice model simulations. *J. Chem. Phys.* **101**, 6052–6062 (1994).
59. Saven, J. G., Wang, J. & Wolynes, P. G. Kinetics of protein folding: the dynamics of globally connected rough energy landscapes with biases. *J. Chem. Phys.* **101**, 11037–11043 (1994).
60. Wang, J., Onuchic, J. & Wolynes, P. G. Statistics of kinetic pathways on biased rough energy landscapes with applications to protein folding. *Phys. Rev. Lett.* **76**, 4861–4864 (1996).
61. Plotkin, S. S., Wang, J. & Wolynes, P. G. Correlated energy landscape model for finite, random heteropolymers. *Phys. Rev. E* **53**, 6271–6296 (1996).
62. Becker, O. M. & Karplus, M. The topology of multidimensional potential energy surfaces: theory and application to peptide structure and kinetics. *J. Chem. Phys.* **106**, 1495–1517 (1997).
63. Dill, K. A. & Chan, H. S. From Levinthal to pathways and funnels. *Nature Struct. Biol.* **4**, 10–19 (1997).
64. Klepeis, J. L., Floudas, C. A., Morikis, D. & Lambris, J. D. Predicting peptide structure using NMR data and deterministic global optimization. *J. Comp. Chem.* **20**, 1354–1370 (1999).
65. Lacks, D. J. Localized mechanical instabilities and structural transformations in silica glass under high pressure. *Phys. Rev. Lett.* **80**, 5385–5388 (1998).
66. Malandro, D. L. & Lacks, D. J. Volume dependence of potential energy landscapes in glasses. *J. Chem. Phys.* **107**, 5804–5810 (1997).
67. Malandro, D. L. & Lacks, D. J. Relationships of shear-induced changes in the potential energy landscape to the mechanical properties of ductile glasses. *J. Chem. Phys.* **110**, 4593–4601 (1999).
68. Malandro, D. L. & Lacks, D. J. Molecular-level instabilities and enhanced self-diffusion in flowing liquids. *Phys. Rev. Lett.* **81**, 5576–5579 (1998).
69. Schulz, M. Energy landscape, minimum points, and non-Arrhenius behavior of supercooled liquids. *Phys. Rev. B* **57**, 11319–11333 (1998).
70. Sastry, S., Debenedetti, P. G. & Stillinger, F. H. Signatures of distinct dynamical regimes in the energy landscape of a glass-forming liquid. *Nature* **393**, 554–557 (1998).
71. Keyes, T. Dependence of supercooled liquid dynamics on elevation in the energy landscape. *Phys. Rev. E* **59**, 3207–3211 (1999).
72. Debenedetti, P. G., Stillinger, F. H., Truskett, T. M. & Roberts, C. J. The equation of state of an energy landscape. *J. Phys. Chem. B* **103**, 7390–7397 (1999).
73. Jonsson, H. & Andersen, H. C. Icosahedral ordering in the Lennard-Jones crystal and glass. *Phys. Rev. Lett.* **60**, 2295–2298 (1988).
74. Angelani, L., Di Leonardo, R., Ruocco, G., Scala, A. & Sciortino, F. Saddles in the energy landscape probed by supercooled liquids. *Phys. Rev. Lett.* **85**, 5356–5359 (2000).
75. Stillinger, F. H., Debenedetti, P. G. & Sastry, S. Resolving vibrational and structural contributions to isothermal compressibility. *J. Chem. Phys.* **109**, 3983–3988 (1998).
76. Stillinger, F. H. & Debenedetti, P. G. Distinguishing vibrational and structural equilibration contributions to thermal expansion. *J. Phys. Chem. B* **103**, 4052–4059 (1999).
77. Sciortino, F., Kob, W. & Tartaglia, P. Inherent structure entropy of supercooled liquids. *Phys. Rev. Lett.* **83**, 3214–3217 (1999).
78. Büchner, S. & Heuer, A. Potential energy landscape of a model glass former: thermodynamics, anharmonicities, and finite size effects. *Phys. Rev. E* **60**, 6507–6518 (1999).
79. Scala, A., Starr, F. W., La Nave, E., Sciortino, F. & Stanley, H. E. Configurational entropy and diffusivity in supercooled water. *Nature* **406**, 166–169 (2000).
80. Prielmeier, F. X., Lang, E. W., Speedy, R. J. & Lüdemann, H.-D. Diffusion in supercooled water to 300 Mpa. *Phys. Rev. Lett.* **59**, 1128–1131 (1987).
81. Mackenzie, J. D. Viscosity-temperature relationship for network liquids. *J. Am. Ceram. Soc.* **44**, 598–601 (1961).
82. Greet, R. J. & Turnbull, D. Glass transition in o-terphenyl. *J. Chem. Phys.* **46**, 1243–1251 (1967).
83. Stillinger, F. H. & Hodgdon, J. A. Translation-rotation paradox for diffusion in fragile glass-forming liquids. *Phys. Rev. E* **50**, 2064–2068 (1994).
84. Tarjus, G. & Kivelson, D. Breakdown of the Stokes-Einstein relation in supercooled liquids. *J. Chem. Phys.* **103**, 3071–3073 (1995).
85. Liu, C. Z.-W. & Openheim, I. Enhanced diffusion upon approaching the kinetic glass transition. *Phys. Rev. E* **53**, 799–802 (1996).
86. Geszti, T. Pre-vitrification by viscosity feedback. *J. Phys. C* **16**, 5805–5814 (1983).
87. Bengtzelius, U., Götz, W. & Sjölander, A. Dynamics of supercooled liquids and the glass transition. *J. Phys. C* **17**, 5915–5934 (1984).
88. Götz, W. & Sjögren, L. Relaxation processes in supercooled liquids. *Rep. Prog. Phys.* **55**, 241–376 (1992).
89. Götz, W. & Sjögren, L. The mode coupling theory of structural relaxations. *Transp. Theory Stat. Phys.* **24**, 801–853 (1995).
90. Götz, W. Recent tests of the mode-coupling theory for glassy dynamics. *J. Phys. Cond. Matt.* **11**, A1–A45 (1999).
91. Kob, W. Computer simulations of supercooled liquids and glasses. *J. Phys. Cond. Matt.* **11**, R85–R115 (1999).
92. Kob, W. & Andersen, H. C. Testing mode-coupling theory for a supercooled binary Lennard-Jones mixture: the van Hove correlation function. *Phys. Rev. E* **51**, 4626–4641 (1995).
93. Kivelson, D., Kivelson, S. A., Zhao, X., Nussinov, Z. & Tarjus, G. A thermodynamic theory of supercooled liquids. *Physica A* **219**, 27–38 (1995).
94. Kivelson, D. & Tarjus, G. SuperArrhenius character of supercooled glass-forming liquids. *J. Non-Cryst. Solids* **235–237**, 86–100 (1998).
95. Kivelson, D. & Tarjus, G. The Kauzmann paradox interpreted via the theory of frustration-limited domains. *J. Chem. Phys.* **109**, 5481–5486 (1998).
96. Sastry, S. The relationship between fragility, configurational entropy and the potential energy landscape of glass-forming liquids. *Nature* **409**, 164–167 (2001).
97. Speedy, R. J. Relations between a liquid and its glasses. *J. Phys. Chem. B* **103**, 4060–4065 (1999).
98. Keyes, T. Instantaneous normal mode approach to liquid state dynamics. *J. Phys. Chem. A* **101**, 2921–2930 (1997).
99. Kirkpatrick, T. R. & Wolynes, P. G. Stable and metastable states in mean-field Potts and structural glasses. *Phys. Rev. B* **36**, 8552–8564 (1987).
100. Kirkpatrick, T. R., Thirumalai, D. & Wolynes, P. G. Scaling concepts for the dynamics of viscous liquids near an ideal glassy state. *Phys. Rev. A* **40**, 1045–1054 (1989).
101. Mézard, M. & Parisi, G. Thermodynamics of glasses: a first principles computation. *Phys. Rev. Lett.* **82**, 747–750 (1999).
102. Berendsen, H. J., Grigera, J. R. & Stroatsma, T. P. The missing term in effective pair potentials. *J. Phys. Chem.* **91**, 6269–6271 (1987).
103. Stillinger, F. H. Supercooled liquids, glass transitions, and the Kauzmann paradox. *J. Chem. Phys.* **88**, 7818–7825 (1988).
104. Santen, L. & Krauth, W. Absence of thermodynamic phase transition in a model glass former. *Nature* **405**, 550–551 (2000).
105. Wilks, J. *The Properties of Liquid and Solid Helium* (Clarendon, Oxford, 1967).
106. Rastogi, S., Höhne, G. W. H. & Keller, A. Unusual pressure-induced phase behavior in crystalline Poly(4-methylpentene-1): calorimetric and spectroscopic results and further implications. *Macromolecules* **32**, 8897–8909 (1999).
107. Greer, A. L. Too hot to melt. *Nature* **404**, 134–135 (2000).
108. Stillinger, F. H. Exponential multiplicity of inherent structures. *Phys. Rev. E* **59**, 48–51 (1999).
109. Stillinger, F. H. Enumeration of isobaric inherent structures for the fragile glass former o-terphenyl. *J. Phys. Chem. B* **102**, 2807–2810 (1998).

#### Acknowledgements

P.G.D.'s work is supported by the US Department of Energy.

Reproduced with permission of the copyright owner. Further reproduction prohibited without permission.